

## Designing porosity and topography of poly(1,3-trimethylene carbonate) scaffolds

Bernke J. Papenburg<sup>a</sup>, Sigrid Schüller-Ravoo<sup>b</sup>, Lydia A.M. Bolhuis-Versteeg<sup>a</sup>, Liesbeth Hartsuiker<sup>a</sup>, Dirk W. Grijpma<sup>b,c</sup>, Jan Feijen<sup>b</sup>, Matthias Wessling<sup>a</sup>, Dimitrios Stamatialis<sup>a,\*</sup>

<sup>a</sup> Membrane Science and Technology, Faculty of Science and Technology, Institute for Biomedical Technology, University of Twente, P.O. Box 217, 7500 AE Enschede, The Netherlands

<sup>b</sup> Polymer Chemistry and Biomaterials, Faculty of Science and Technology, Institute for Biomedical Technology, University of Twente, P.O. Box 217, 7500 AE Enschede, The Netherlands

<sup>c</sup> Department of Biomedical Engineering, University Medical Center Groningen, University of Groningen, Antonius Deusinglaan 1, 9713 AV Groningen, The Netherlands

Received 30 January 2009; received in revised form 2 April 2009; accepted 12 May 2009

Available online 20 May 2009

### Abstract

Using phase separation micromolding (PS $\mu$ M) we developed porous micro-patterned sheets from amorphous poly(1,3-trimethylene carbonate) (PTMC). The use of these PTMC sheets can be advantageous in tissue engineering applications requiring highly flexible constructs. Addition of poly(ethylene oxide) (PEO) in various amounts to PTMC casting solutions provides PTMC sheets with tailored porosity and pore sizes in the range 2–20  $\mu$ m. The pore-forming effect of PEO during the phase separation process is evaluated and glucose transport measurements show that the pores are highly interconnected. Additionally, tailoring the micro-pattern design yields PTMC sheets with various surface topographies. Cell culturing experiments with C2C12 pre-myoblasts revealed that cell attachment and proliferation on these sheets is relatively high and that the micro-pattern topography induces a clearly defined cell organization.

© 2009 Acta Materialia Inc. Published by Elsevier Ltd. All rights reserved.

**Keywords:** Tissue engineering scaffold; Phase separation; Micro-patterning; Poly(trimethylene carbonate); Cell attachment and proliferation

### 1. Introduction

In tissue engineering the choice of scaffold material plays an important role in the functionality of the designed scaffold for various applications. Characteristics of the material should correspond to the required properties at the site of implantation, e.g. suitable flexibility, mechanical strength and degradation in pace with tissue growth [1,2].

Amongst synthetic biodegradable biomaterials poly(lactic acid) (PLA) and poly(glycolic acid) (PGA) and their

co-polymers have been intensively studied [3,4]. However, the stiffness and degradation profiles of these materials can be unfavorable, especially when considering certain soft tissue engineering applications. Poly(1,3-trimethylene carbonate) (PTMC) is a good alternative material in these cases, due to its elasticity combined with slow degradation in aqueous solutions and rapid degradation *in vivo* via enzymatic degradation without leading to the formation of acidic products, as in the case of, for example, PLA [5,6]. Also, selecting high molecular weight PTMCs yields relatively good mechanical properties [7]. Alternatively, one can synthesize co-polymers of PTMC with other polymers, e.g. PLA and poly( $\epsilon$ -caprolactone) (PCL), to obtain

\* Corresponding author. Tel.: +31 53 4894675; fax: +31 53 4894611.

E-mail address: [d.stamatialis@utwente.nl](mailto:d.stamatialis@utwente.nl) (D. Stamatialis).

a co-polymer that has improved flexibility and degradation properties compared with, for example, PLA and an increased Young modulus compared with PTMC [8–11]. *In vivo* studies using PTMC-based scaffolds have revealed the suitability of these materials for application in, for example, protein delivery systems [12] and the prevention of post-operative adhesions [13].

Besides the choice of material, scaffold design is very important for the functionality of the engineered tissue [2,14]. One of the most important requirements is ensuring a good nutrient supply to the cells, which can be achieved via scaffold inner porosity. Another important issue is cell organization, which can be influenced by varying the scaffold topography. In this way, the organization of the cells can be tuned, thereby improving the functionality of the grown tissue [15,16].

In a previous work we showed that phase separation micromolding (PS $\mu$ M) enables fabrication of porous micro-patterned sheets that can be stacked into three-dimensional scaffolds [17]. Various polymers, such as poly(L-lactic acid) (PLLA), poly(D,L-lactic acid) (PDLA) and poly( $\epsilon$ -caprolactone) (PCL), were processed and the most suitable PLLA fabricated sheets were selected to analyze the functionality of the micro-patterned porous sheets as scaffold sheets.

In this work we used PS $\mu$ M to fabricate porous micro-patterned PTMC scaffold sheets. Porosity was introduced and tuned by adding various amounts of poly(ethylene oxide) (PEO) to PTMC casting solutions. The pore forming effect of PEO during the phase separation process of the PTMC sheets was studied and various micro-patterned PTMC sheets were manufactured by casting on properly designed molds. Micro-pattern replication and pattern and morphology stability of these PTMC sheets were studied systematically. We successfully fabricated micro-patterned porous PTMC sheets that supported cell attachment, proliferation and morphology very well.

## 2. Materials and methods

### 2.1. PTMC synthesis and characterization

PTMC synthesis is slightly modified with respect to previously reported protocols [7,11]. Briefly, in an argon atmosphere a freshly silanized dried glass ampoule (silanized with SERVA silicone solution in isopropanol; SERVA Electrophoresis GmbH, Heidelberg, Germany) was charged with trimethylene carbonate (TMC) (1,3-dioxan-2-one) monomer (polymer grade; Boehringer Ingelheim) and  $1.8 \times 10^{-4}$  mol stannous octoate catalyst (stannous 2-ethylhexanoate, SnOct<sub>2</sub>; Sigma) per mol monomer was added. The ampoule was purged three times with dry argon, heat-sealed under vacuum and conditioned in a pre-heated oil bath. To ensure homogeneous mixing of monomer and catalyst the ampoule was shaken vigorously for the first hour of reaction. Polymerization was carried out at 130 °C for 3 days. To purify the obtained polymer

was dissolved in chloroform (2% w/v solution, analytical quality; Merck), filtered and precipitated into a fivefold volume of ethanol (analytical quality, Merck). Subsequently, the precipitated polymer was collected and dried prior to use.

Monomer conversion of the synthesized polymer was characterized by nuclear magnetic resonance (NMR) spectroscopy. <sup>1</sup>H NMR (Varian Unity 300 MHz) spectra were recorded using solutions of the polymer in deuterated chloroform (CDCl<sub>3</sub>; Merck).

The molecular weight, molecular weight distribution and intrinsic viscosity of PTMC were determined by gel permeation chromatography (GPC) using chloroform (p.a., filtered through a 0.2  $\mu$ m Whatman Schleicher & Schuell RC58 membrane filter prior to use) as eluent. The GPC set-up consisted of a GPCmax VE-2001 GPC solvent/sample module, a series of ViscoGEL I columns and a TDA 302 triple detector array comprising a light scattering detector (RALS and LALS), a differential refractive index detector and a four-capillary differential viscometer. A polystyrene standard ( $M_n = 6.4 \times 10^4$  g mol<sup>-1</sup>) with a narrow molecular weight distribution was used for calibration.

Thermal properties of the pure polymers and their blends were evaluated by differential scanning calorimetry (DSC) using a Perkin Elmer Pyris1 (USA). Samples of 5–10 mg were heated from –100 °C to 100 °C at a heating rate of 10 °C min<sup>-1</sup>. The glass transition temperature ( $T_g$ ) was obtained from the midpoint of the heat capacity change and the melting range and peak temperature ( $T^m$ ) were determined from the melting endotherm. Cyclohexane, indium and lead were used as standards for temperature calibration.

### 2.2. Scaffold preparation

PS $\mu$ M, which was used as the fabrication method, has been described in detail in previous works [17,18].

#### 2.2.1. PTMC

In this study the synthesized high molecular weight PTMC was dissolved in chloroform (analytical grade; Merck) at a concentration of 3 wt.%. In order to prepare porous PTMC sheets PEO ( $M_w$   $6 \times 10^6$  g mol<sup>-1</sup>; Aldrich) was added to the 3 wt.% PTMC–CHCl<sub>3</sub> solution, as PEO is water soluble and can, therefore, be leached out after the phase separation process. Concentrations varying from 0.1 to 1.0 wt.% with respect to the total final casting solution were used. Table 1 gives an overview of the various casting solution compositions and the notations that will be used from this point on. The polymer solutions were cast on flat or micro-patterned molds to obtain non-patterned or micro-patterned sheets, respectively. Two micro-pattern designs were applied, which are illustrated in Fig. 1. Table 2 lists their dimensions. A mixture of ethanol (analytical grade; Merck,) and Milli-Q water at a ratio of 8:1 at room temperature (ranging from 18 to 21 °C) was

Table 1  
Composition of PTMC casting solutions.

Notation	Polymer content (g)			Chloroform content (g)
	PTMC	PEO	Total	
Dense/0 wt.% PEO	3	0	3.0	97.0
0.1 wt.% PEO	3	0.1	3.1	96.9
0.3 wt.% PEO	3	0.3	3.3	96.7
0.5 wt.% PEO	3	0.5	3.5	96.5
0.75 wt.% PEO	3	0.75	3.75	96.25
1.0 wt.% PEO	3	1.0	4.0	96.0

used as non-solvent. All sheets were cast with an initial casting thickness of 500  $\mu\text{m}$ . After casting the sheets were left in the non-solvent for 1 day to leach out the PEO. Subsequently, the sheets were washed in Milli-Q water for 1–3 days and dried in a temperature controlled atmosphere (18–21  $^{\circ}\text{C}$ ). Sheets used in cell culture experiments were conditioned in culture medium at 4  $^{\circ}\text{C}$  (C2C12 proliferation medium; for composition see Cell culturing) for up to 5 h before washing with Milli-Q water and drying. To preserve the porous morphology the non-solvent and washing bath were kept at 4  $^{\circ}\text{C}$  and after drying the sheets were stored at  $-20^{\circ}\text{C}$ .

### 2.2.2. PLLA

Porous and dense PLLA sheets were used as references in the cell culture experiments. Porous PLLA sheets were prepared from 5 wt.% PLLA ( $M_w$   $1.6 \times 10^5 \text{ g mol}^{-1}$ ,  $M_n$   $8.4 \times 10^4 \text{ g mol}^{-1}$ ) in 1,4-dioxane, using ethanol at 3–4  $^{\circ}\text{C}$  as non-solvent. Dense PLLA sheets were prepared from 10 wt.% PLLA in chloroform (analytical grade; Merck), left to evaporate for 30–60 s and placed in a non-solvent bath of ethanol at room temperature. Both dense and porous PLLA sheets were left in the non-solvent bath for 1 day to ensure full removal of the solvent and subsequently washed for 5–8 h in Milli-Q water, which was refreshed 2–3 times, and subsequently dried in a controlled atmosphere (temp. 18–21  $^{\circ}\text{C}$ ).

### 2.3. PEO content

To determine the amount of PEO remaining in the PTMC sheets after phase separation, washing and drying  $^1\text{H}$  NMR spectra were recorded for sheets cast from

0.5 wt.% PEO casting solutions. A similar sheet was cast and, after phase separation, washed for only 3 h. Another 0.5 wt.% PEO sheet was cast but instead of solvent/non-solvent exchange, the sheet was left in a controlled atmosphere overnight for complete chloroform evaporation. One part of this sheet was stored until measured while another part was washed in Milli-Q water for 3 h and the last part was washed in Milli-Q water for 3 days before drying.  $^1\text{H}$  NMR spectra were also recorded for these three sheets, as well as for pure PTMC and PEO controls.

### 2.4. Porosity and pore morphology

To study sheet morphology, porosity and pore size range image analysis using scanning electron microscopy (SEM) (JEOL 5600LV) was performed on gold coated ( $\sim 15 \text{ nm}$  thick layer) samples. Porosity was calculated from weight, volume (thickness was determined from the SEM images) and density as described in a previous work [17] and the pore size range was based on the SEM images. As an indication of pore interconnectivity and nutrient transport through the sheets diffusion of glucose through the sheets was measured using the set-up described in detail elsewhere [17]. Basically, sheets are placed between a donor and an acceptor compartment and the transport of glucose from the donor to the acceptor side was measured over a surface area of  $0.50 \text{ cm}^2$ . From the change on the concentrations over time the glucose diffusion coefficient was calculated. For these experiments a 10-fold higher glucose concentration than that in blood was used ( $10 \text{ g l}^{-1}$ ,  $57 \text{ mmol l}^{-1}$ ) (D(+)-glucose, 99.5% GC, SigmaUltra) in Milli-Q water. Samples of 0.15 ml were taken at various time points from both the donor and acceptor compartments, at 0 and 30 min and 1, 2, 3, 4, 5, 8 and 24 h. For the porous sheets additional samples were taken at 5, 10 and 15 min. The glucose concentrations in the donor and acceptor compartments were determined for triplicate sheets by an enzymatic assay according to the manufacturer's protocol (PGO enzymes; Sigma). The enzymatic reaction with glucose produces orange coloured solutions which were analyzed by UV spectrophotometry (Varian Cary 300 scan) at  $\lambda = 450 \text{ nm}$ .

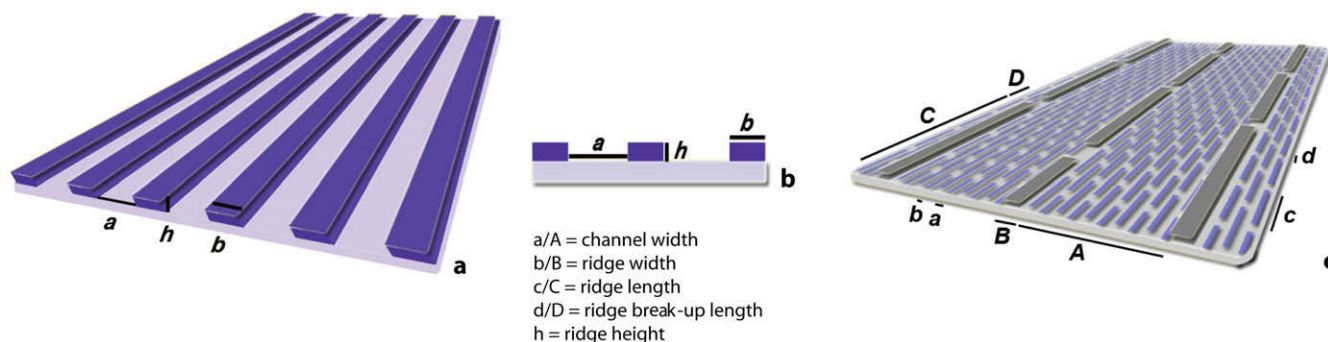


Fig. 1. Schematic illustration of the mold designs: (a) top view of channel pattern; (b) side view of channel pattern; (c) double pattern with larger and smaller channels that are both periodically broken up (referred to as the double brick pattern).

Table 2  
Specifications of micro-pattern dimensions for both molds and corresponding PTMC sheets cast from various solutions.

Pattern feature		Mold ( $\mu\text{m}$ )	Density ( $\mu\text{m}$ )	0.5 wt.% PEO ( $\mu\text{m}$ )	1 wt.% PEO ( $\mu\text{m}$ )
Double brick	A, a	300, 20	160, 7	220, 11	170, 10
	B, b	50, 10	21, 8	27, 7	28, 7
	C, c	500, 100	210, 35	320, 60	285, 55
	D, d	150, 10	120, 21	140, 8	100, 8
	H, h	100, 15	$\sim 35, \sim 8$	40, 10	40, 10
25 $\mu\text{m}$ channel	a	25	10	25	$\sim 15$
	b	25	15	15	$\sim 20$
	h	30	9	10	$\sim 10$

A represents the channel width, B the ridge width, C the ridge length until interconnection, D the ridge interconnection length and H the ridge height, as also illustrated in Fig. 1. For the double brick pattern upper case letters refer to the larger pattern, while the lower case letters refer to the smaller pattern.

## 2.5. Sheet morphology under physiological conditions

Change of morphology over time of PTMC sheets cast from 0.5 and 1 wt.% PEO solutions was studied under physiological conditions, simulated by placing the sheets either in PBS or in culture medium (C2C12 proliferation medium, see below) at 37 °C in a humid atmosphere containing 5% CO<sub>2</sub>. Triplicate samples with a diameter of 15 mm were taken at various time points: 0 (control), 4 and 8 h, 1, 2 and 4 days and 1, 2, 3 and 4 weeks. Sheet morphology was determined by SEM imaging.

Some PTMC sheets were cross-linked using  $\gamma$ -irradiation (50 kGy, performed at Isotron Nederland BV, Ede, The Netherlands) while being kept under vacuum in 24-well plates (Nunc).

## 2.6. Cell culture

Cell culture experiments were performed using mouse C2C12 pre-myoblasts to study cell attachment, proliferation and morphology on the PTMC sheets. In some cases PLLA sheets were used as a reference material. For all cell culture experiments sheets were placed in 24-well plates (Nunc) and performed in triplicate unless stated otherwise. To prevent the sheets floating in the wells o-rings (Viton type 51414, 14  $\times$  1 mm; Eriks, The Netherlands) of exactly the same size as the inner diameter of the well were placed on top of the sheets.

C2C12 cells were cultured in proliferation medium containing Dulbecco's-modified Eagle's medium (D-MEM) (Gibco) supplemented with 10% fetal bovine serum (FBS) (Cambrex), 100 U ml<sup>-1</sup> penicillin (Gibco) and 100  $\mu\text{g}$  ml<sup>-1</sup> streptomycin (Gibco). Cells were grown at 37 °C in a humid atmosphere containing 5% CO<sub>2</sub>. Medium was refreshed every 2 or 3 days. For proliferation studies the cells were plated at 2000–3000 cells cm<sup>-2</sup> until they reached  $\sim 80\%$  confluence, then they were detached by trypsinization (0.05% trypsin containing 1 mM EDTA) and further sub-cultured or used for seeding on the polymer sheets at a density of 15,000 cells cm<sup>-2</sup> (unless stated otherwise). Cell numbers were determined by manual counting using a hemacytometer.

## 2.7. Cell culture analysis

### 2.7.1. Fixation and staining for light microscopy

After the medium was aspirated from the wells the sheets cultured with cells were incubated in 4% paraformaldehyde (Merck) in PBS for 30–60 min to fixate the cells. Subsequently, the sheets were washed with PBS and a few drops of methylene blue (1% in borax) solution were added for 3–5 min to stain the cells. Then the sheets were thoroughly washed with demineralized water to ensure full removal of all excess methylene blue. The sheets were stored in PBS at 4 °C until time of measurement (within 1 week). Images were taken using light microscopy (Zeiss Axiovert 40 mat and AxioCam MRC 5 camera).

### 2.7.2. Attachment

Attachment of the cells onto the sheets was determined 4 h post-seeding by aspirating the seeding suspension and manually counting the number of cells in this suspension. Cell attachment was calculated by the total number of cells seeded minus the number of cells counted in the seeding suspension after 4 h attachment.

### 2.7.3. Proliferation—trypan blue exclusion

Proliferation of cells after 4 and 8 days was determined using trypan blue exclusion with manual counting. Cells were detached from the sheets by trypsinization, the cell suspension was aspirated and trypan blue (0.4% solution; Sigma) was added in a 1:1 ratio before counting. Statistical significance was calculated using Student's *t*-test at  $P < 0.05$ .

### 2.7.4. Proliferation—DNA assay

A DNA assay was performed to determine the total concentration of DNA per sample to determine cell proliferation on the various sheets. After washing the sheets with PBS the cells were lysed (cell culture lysis reagent E153A, Promega) and DNA concentrations were measured using a cell proliferation assay according to the manufacturer's protocol (CyQuant Cell Proliferation Assay Kit; Invitrogen/Molecular Probes). Statistical significance was calculated using Student's *t*-test at  $P < 0.05$ .

### 2.7.5. Quantitative RT-PCR

To analyze gene expression the quantitative reverse transcriptase-polymerase chain reaction (RT-PCR) method was used to determine myogenic differentiation of C2C12 cells using the early and late markers myoD and myogenin (primer assays for mouse MyoD1 and MyoG; SABiosciences, Frederick, MD); expression was corrected for murine glyceraldehyde 3-phosphate dehydrogenase (Mus GAPDH, forward 5'-AACGACCCCTTCATTGAC-3', reverse 5'-TCCACGACATACTCAGCAC-3'). To obtain enough RNA the surface area of the sheets was increased. Therefore, the sheets were placed in 12-well plates (Nunc) and o-rings of size  $19.5 \times 1$  mm were placed on top to prevent floating. C2C12 cells were seeded at a density of  $15,000 \text{ cells cm}^{-2}$  and cultured in triplicate for 4 and 8 days. Medium was refreshed every 2 days. On days 4 and 8 cells on the respective sheets were detached by trypsinization and pellets were prepared. RNA was isolated from the pellets using a Qiagen RNeasy kit (Qiagen, Chatsworth, CA) following the manufacturer's protocol. RNA concentration and quality was determined by the Nanodrop method and quality was also confirmed by running the RNA on a 1% w/v agarose gel by electrophoresis. A sample of  $1 \mu\text{g}$  RNA was synthesized into cDNA using Superscript II (Invitrogen, Calsbad, CA) according to the manufacturer's protocol. A sample of  $1 \mu\text{l}$  cDNA was used with  $0.5 \mu\text{M}$  primer in SYBR Green I master mix (Invitrogen) and gene expression was determined by real time quantitative PCR (Bio-Rad iCycler) (40 cycles, melting 15 s at  $95^\circ\text{C}$ , annealing 30 s at  $55^\circ\text{C}$  and extension 30 s at  $72^\circ\text{C}$ ). Expression of the myoD and myogenin genes was calculated relative to GAPDH housekeeping gene levels by the  $2^{-\Delta\Delta C_T}$  method [19] and statistical significance was calculated using Student's *t*-test at  $P < 0.05$ .

## 3. Results and discussion

### 3.1. PTMC synthesis and characterization

The synthesized PTMC had an average  $M_n$  of  $2.66 \times 10^5 \text{ g mol}^{-1}$  and shows a polydispersity index (PDI) of 1.39 and an intrinsic viscosity of  $3.75 \text{ dl g}^{-1}$ . More details on the thermal and mechanical properties of PTMC were reported earlier by Pêgo et al. [7]. DSC data for the sheets prepared with PEO confirmed the presence of two separate phases, one corresponding to PTMC ( $T_g = -17^\circ\text{C}$ ) and one corresponding to PEO ( $T_g = -56^\circ\text{C}$ ), in agreement with the DSC results for the pure components ( $T_g = -16$  and  $-51^\circ\text{C}$ , respectively).

### 3.2. PTMC scaffold preparation

#### 3.2.1. Shrinkage and micro-pattern replication

The polymer sheets shrank extensively during the fabrication process; the sheets cast without PEO shrank up to 200–300%, whereas the sheets with PEO shrank up to 130–180%. Although shrinkage influenced the final dimen-

sions of the micro-pattern imprinted into the sheets, replication of the features of both molds applied was good. Micro-pattern replication in various sheets can also be observed in the SEM images presented in Fig. 2, which will be described in more detail in the next paragraph.

There is some variation in the quality and size of the imprinted micro-pattern. Table 2 lists the original feature dimensions and the final dimensions of the imprinted features of sheets prepared with 0, 0.5 and 1 wt.% PEO for both the  $25 \mu\text{m}$  channel and double brick patterns. The sheets experiencing most shrinkage, i.e. those without PEO, also showed the highest variance in feature dimensions, as would be expected. Apart from the influence on feature dimensions, the sheets prepared with 0.5 and 1 wt.% PEO displayed large surface pores that affected the micro-pattern to a certain extent. This effect was especially apparent for the 1 wt.% PEO sheets, including the double brick pattern. In any case, shrinkage can be taken into account when designing molds to obtain sheets with the desired final dimensions.

Finally, it is important to note that handling these thin PTMC sheets ( $<30 \mu\text{m}$ ) was often difficult due to their flexibility and stickiness. Conditioning of the sheets in culture medium improved handling by decreasing the “stickiness” of the sheets.

### 3.3. Porosity and pore morphology

#### 3.3.1. Porosity and additive concentration

Dense sheets were obtained using a 3 wt.% polymer solution of PTMC in chloroform. To introduce porosity PEO was used as an additive at various concentrations (Table 1). Fig. 2 shows SEM images of sheets prepared with increasing concentrations of PEO in the casting solution; for each sheet type the porosity and pore size range are also presented. Both porosity and pore size increased as the PEO concentration in the casting solution increased to 0.5 wt.%. Above this value both porosity and pore size were almost constant (within the measured range). Sheets cast from solutions with 0.1 and 0.3 wt.% PEO had porosities of 11% and 18%, with a pore size range of 2–10 and 2–15  $\mu\text{m}$ , respectively (Fig. 2b and c). Whereas sheets cast from the 0.5 (Fig. 2d) and 1 wt.% PEO casting solutions (Fig. 2e) yielded porosities of up to 31%, with a pore size range of 5–20  $\mu\text{m}$ . Fig. 2a shows the sheets prepared without addition of PEO.

#### 3.3.2. Role of PEO in pore formation

To fully understand the role of PEO in pore formation and to analyze the influence of the different processing steps, the amount of PEO remaining in the sheets after solidification and washing was determined by  $^1\text{H}$  NMR analysis. Additionally, PTMC sheets cast from 0.5 wt.% PEO casting solution processed in different ways were analyzed by SEM. A number of sheets were phase separated while others were left for the solvent to evaporate after casting to preserve the PEO during solidification. In addition, various washing times were applied.

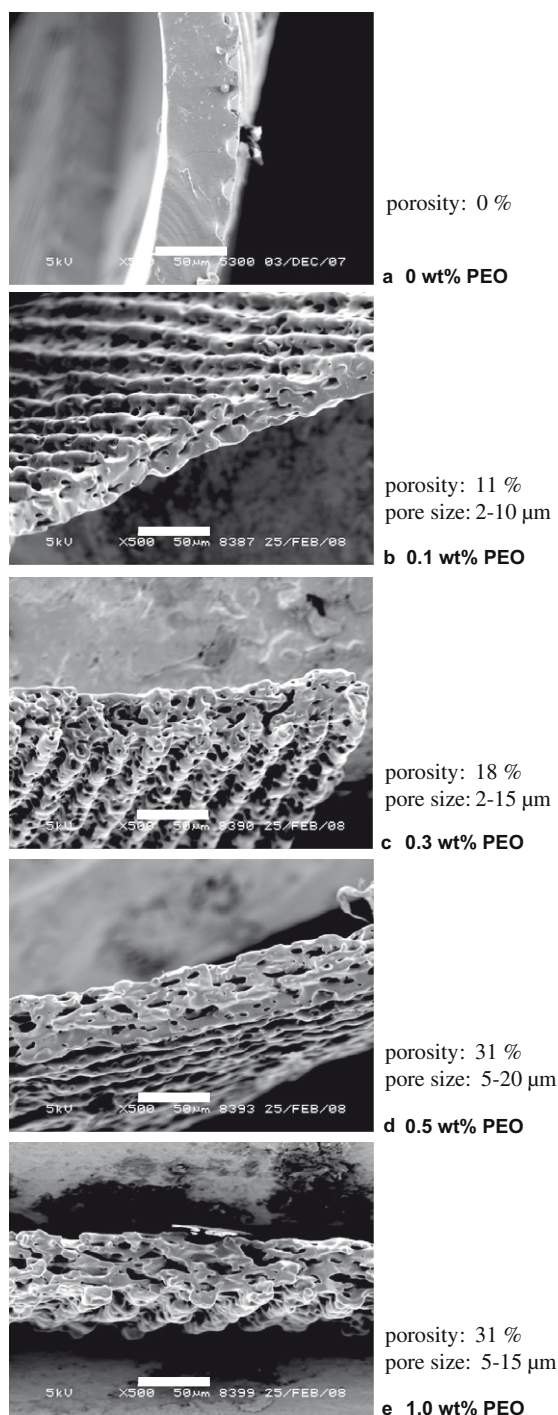


Fig. 2. Typical SEM cross-section images of 25  $\mu\text{m}$  channel featuring sheets cast from 3 wt.% PTMC- $\text{CHCl}_3$  with various amounts of PEO as additive. Amount of PEO with respect to the total weight of the polymer solution: (a) 0 wt.%; (b) 0.1 wt.%; (c) 0.3 wt.%; (d) 0.5 wt.% and (e) 1.0 wt.%. Magnification of all images  $\times 500$ , the bar in the images represents 50  $\mu\text{m}$ .

Fig. 3e and f show the reference  $^1\text{H}$  NMR spectra recorded for pure PEO and pure PTMC, respectively. Fig. 3a–c shows the spectra recorded for the sheets from which solvent was evaporated but that were not washed and those washed for 3 h and for 3 days, respectively. All

these spectra show a clear peak of PEO at 3.65 ppm which decreased significantly when washing was applied. The PEO content in these polymer sheets, calculated from the area under the PEO peak, was 13.4 wt.% when no washing was applied, which is in close agreement with the theoretically expected amount of 14.3 wt.% PEO. After 3 h washing the PEO content was still 9.4 wt.%, and after 3 days 6.7 wt.%. These results clearly indicate that PEO is trapped within the solidified sheet, and washing only leached out up to half of the PEO content. Fig. 3d shows the  $^1\text{H}$  NMR spectrum for the phase separated sheets washed for 3 days, where only a small PEO peak corresponding to 1.3 wt.% PEO was observed. When the phase separated sheets were washed for just 3 h the PEO content was still only 2.0 wt.%. It seems that during phase separation and solvent/non-solvent exchange leaching out of PEO was promoted and only a small amount of PEO was left in the sheets, perhaps as a nanometer thick surface layer. Pêgo et al. suggested that small amounts of PEO remaining on the pore wall might actually have a stabilizing effect and assist porosity preservation, whereas preparation of porous PTMC by NaCl leaching leads to pore collapse during the washing and/or drying process [20].

Fig. 4a and b present SEM images of PTMC sheets from which the solvent had been evaporated without washing, whereas Fig. 4c, d, e and f presents such sheets with washing for 3 h and 3 days, respectively. These images show that pore formation in the sheets from which the solvent had been evaporated was poor and pore morphology was not comparable with the interconnected pores observed for the phase separated sheets as presented in Fig. 2.

These results clearly indicate that PEO does not act only as a pore former or leaching agent, as happens with, for example, salts such as NaCl, but also influences the phase separation process itself. The role of high molecular weight PEO in the PTMC–chloroform system seems to resemble that of the high molecular weight additive poly(vinyl pyrrolidone) (PVP) in the preparation of porous membranes of amorphous poly(ether sulfone) (PES) [21]. There it was suggested that during the first moments (fraction of seconds) after immersion diffusion of the solvent and non-solvent is dominant and inter-diffusion of the two polymers (main polymer and additive) could be neglected. Thus, the thermodynamic system can be considered (semi)ternary, with the two polymers regarded as one constituent. On a longer time-scale, inter-diffusion of the polymers becomes more important leading to diffusion into two phases and the system goes from (semi)ternary to quaternary. By this change in system the demixing conditions are changed and instantaneous demixing can occur, leading to the formation of a highly interconnected porous morphology. This phenomenon is in contrast to a more cellular morphology combined with skin formation at the surface in the case of the delayed demixing that might occur in a specific ternary system. Further, with increasing polymer concentration in the polymer-rich phases the viscosity within these phases simultaneously rises to the point of vit-

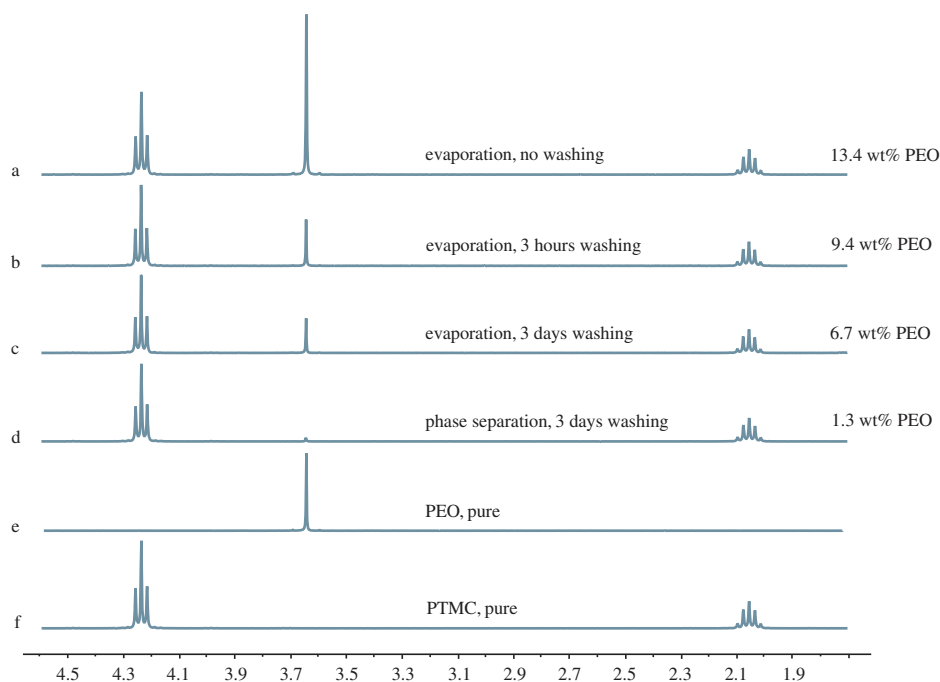


Fig. 3.  $^1\text{H}$  NMR spectra of sheets cast from a 0.5 wt.% PEO solution under various processing conditions: (a–c) evaporation with, subsequently, (a) no washing, (b) washing for 3 h and (c) washing for 3 days; (d) phase separation in non-solvent followed by 3 days washing; (e) pure PEO; (f) pure PTMC, as reference. Peaks represent the  $-\text{CH}_2-\text{O}-$  group of PTMC (4.24 ppm), PEO (3.64 ppm), the  $-\text{CH}_2-$  group of PTMC (2.05 ppm). The chemical shifts of PTMC (4.24 ppm, 4H and 2.05 ppm, 2H) and PEO (3.64 ppm, 4H) are reported against the  $\text{CDCl}_3$  (7.26 ppm) reference.

rification, which is generally considered to finalize the morphology. In most cases vitrification occurs before the final equilibrium is reached and, therefore, some additive polymer will still be present in the main polymer-rich phase and can be permanently entrapped.

Our results seem to be in agreement with this theory, that the phase separation process not only facilitates leaching out of PEO, but that PEO has an additional role as a pore former during phase separation, creating highly interconnected pores, as discussed in the next section.

### 3.3.3. Pore interconnectivity

To determine the interconnectivity of the pores glucose diffusion through the sheets was measured. For dense sheets, prepared without PEO, there was no glucose transport over 24 h. For porous sheets prepared with 0.5 and 1 wt.% PEO, where the pores are 5–20  $\mu\text{m}$ , the glucose transport was equal to the free diffusion coefficient of glucose in water ( $9 \times 10^{-10} \text{ m}^2 \text{ s}^{-1}$ ) [22]. In fact, convective flow of the glucose solution through the sheets was observed while preparing the set-up, showing that these porous sheets have highly interconnected pores despite the relatively moderate porosity of 31%. This high glucose diffusion was remarkable when compared with glucose diffusion through PLLA sheets with porosities of up to 86%, as reported previously [17]. In these systems the highest diffusion coefficient measured was still one order of magnitude lower than that of the PTMC sheets. This result once more highlights the high pore interconnectivity of the PTMC sheets and supports the hypothesis that PEO

induces a change in the thermodynamic system during the phase separation process.

## 3.4. Sheet morphology under physiological conditions

### 3.4.1. Physiological conditions

The degradation properties of high molecular weight PTMC vary greatly depending on the environment. In PBS PTMC degrades very slowly, with a slight decrease in molecular weight and little mass loss over a period of 6 months. In contrast, degradation by enzymatic surface erosion *in vivo* is fast [5,6].

To study the morphology of the processed micro-patterned porous PTMC sheets under physiological conditions the sheets were placed in medium or PBS at 37  $^\circ\text{C}$  and at various time points samples were taken and analyzed. Fig. 5 depicts SEM images of 0.5 wt.% PEO sheets after 1 and 4 weeks in medium and PBS. When placed in medium the walls thickened and the porosity decreased within 1 week (Fig. 5a). This was even more pronounced for sheets in PBS (Fig. 5b). After 4 weeks sheets placed in both medium and PBS had no pores (Fig. 5c and d). Similar phenomena were observed for PTMC sheets with 1 wt.% PEO (data not shown). Since PTMC only has about 1.3% water uptake after 30 days [20], it seems unlikely that swelling causes the change in morphology. It may be envisaged that creep as result of the low  $T_g$  in combination with the low Young's modulus of the PTMC induced loss of porosity over time.

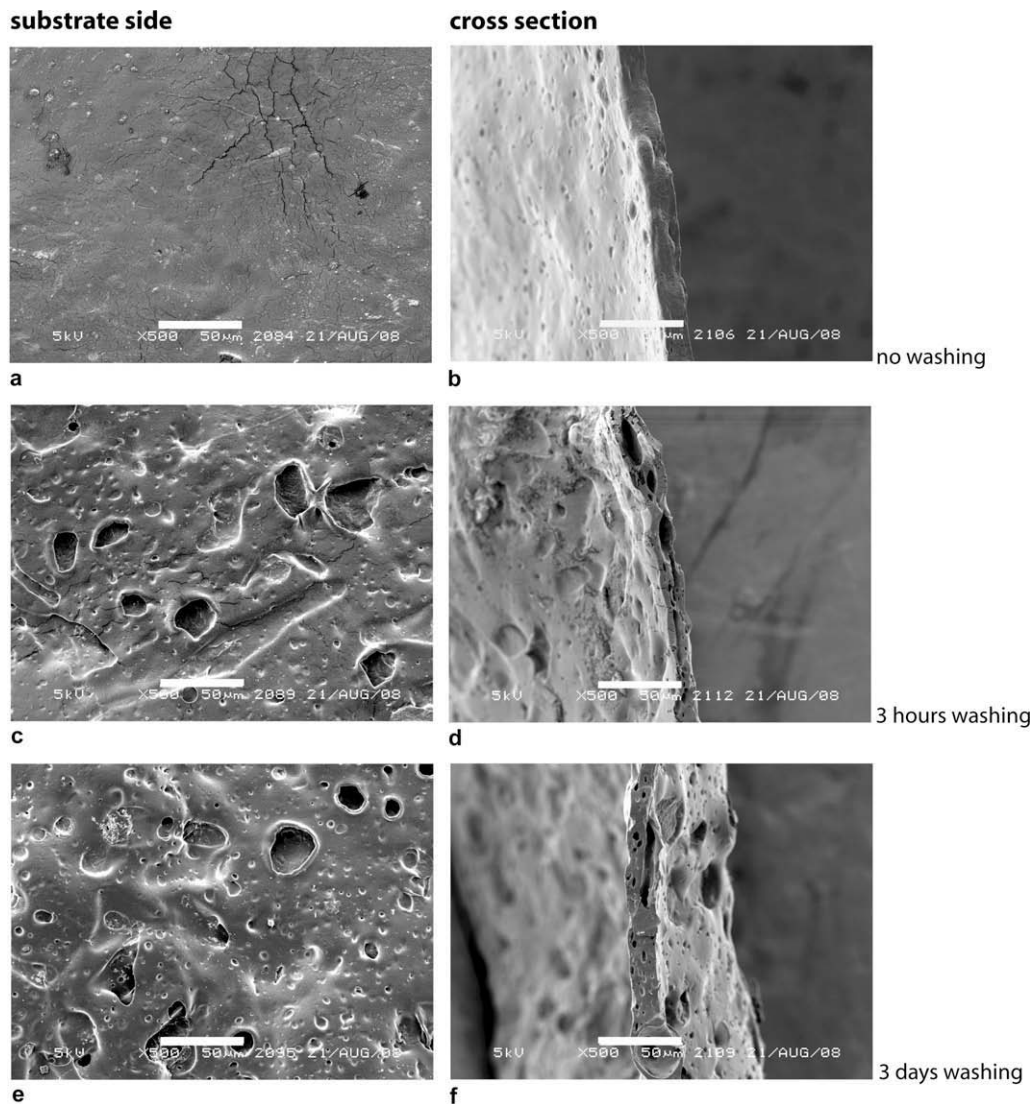


Fig. 4. SEM images of the solvent evaporated sheets cast from a 0.5 wt.% PEO solution of which the  $^1\text{H}$  NMR spectra are represented in Fig. 3. Magnification of all images  $\times 500$ , the bar in the images represents 50  $\mu\text{m}$ .

The porous PTMC sheets also lost their porosity on being  $\gamma$ -irradiated, probably due to the high dose of 50 kGy used in these experiments. Therefore, all sheets were stored at  $-20^\circ\text{C}$  after preparation, as under these conditions the porous morphology of the sheets is preserved without the need for any post-processing. Finally, it is important to note that the stickiness of the thin PTMC sheets was significantly reduced after being submerged in medium, probably due to adsorption of proteins or other compounds present in the medium onto the surface of PTMC sheets.

### 3.5. Cell morphology

Light microscopy images of  $\gamma$ -irradiated PTMC sheets featuring 25  $\mu\text{m}$  wide channels prepared from 0 (Fig. 6a) and 0.5 wt.% PEO (Fig. 6b and c) casting solutions show good alignment of the C2C12 cells to the pattern. For comparison, Fig. 6d and e present the results for PLLA pat-

terned sheets. In both cases (PTMC and PLLA) cell alignment is  $75 \pm 2\%$ , which is in close agreement with earlier results for PLLA:  $81 \pm 5\%$  for a 25  $\mu\text{m}$  channel pattern [17]. Despite similar alignment, the cell morphology on the PTMC sheets appeared different to PLLA. The cells spread more on the PLLA surface, but were highly organized and stretched on the PTMC surfaces. Additionally, the PTMC patterned sheets seem to facilitate fusion of multiple cells (indicated by an arrow in Fig. 6c), a first sign of myogenic differentiation, which is the formation of skeletal muscle tissue by myoblast cells fusing to form multinucleated myotubes [23]. C2C12 cells are known to differentiate into muscle tissue under serum-deprived conditions, but might also differentiate when activated by other environmental cues, e.g. the surface the cells grow on [24,25]. To gain a more detailed look into this phenomenon, cell proliferation on these sheets was examined in relation to entering the myogenic lineage, as the cells exit the cell cycle and proliferation is inhibited [26,27].

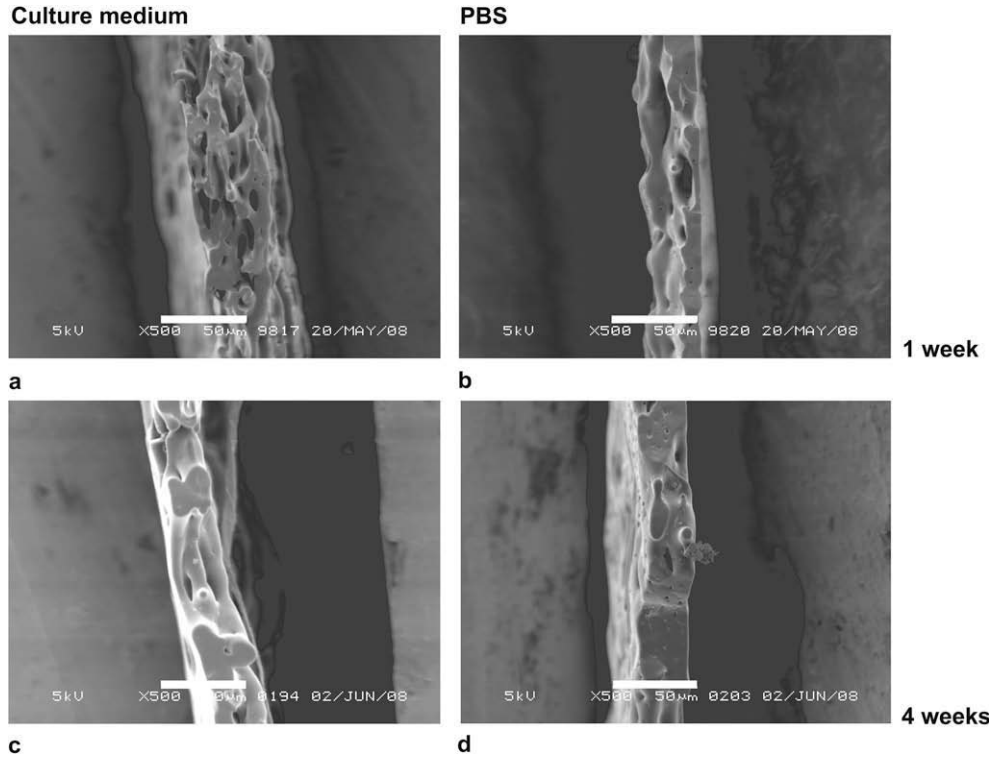


Fig. 5. Typical cross-sectional SEM images of sheets cast from a 0.5 wt.% PEO solution featuring the 25 μm channel pattern in (a and c) medium or (b and d) PBS at 37 °C for 1 (a and b) and 4 (c and d) weeks. Magnification of all images × 500, the bar in the images represents 50 μm.

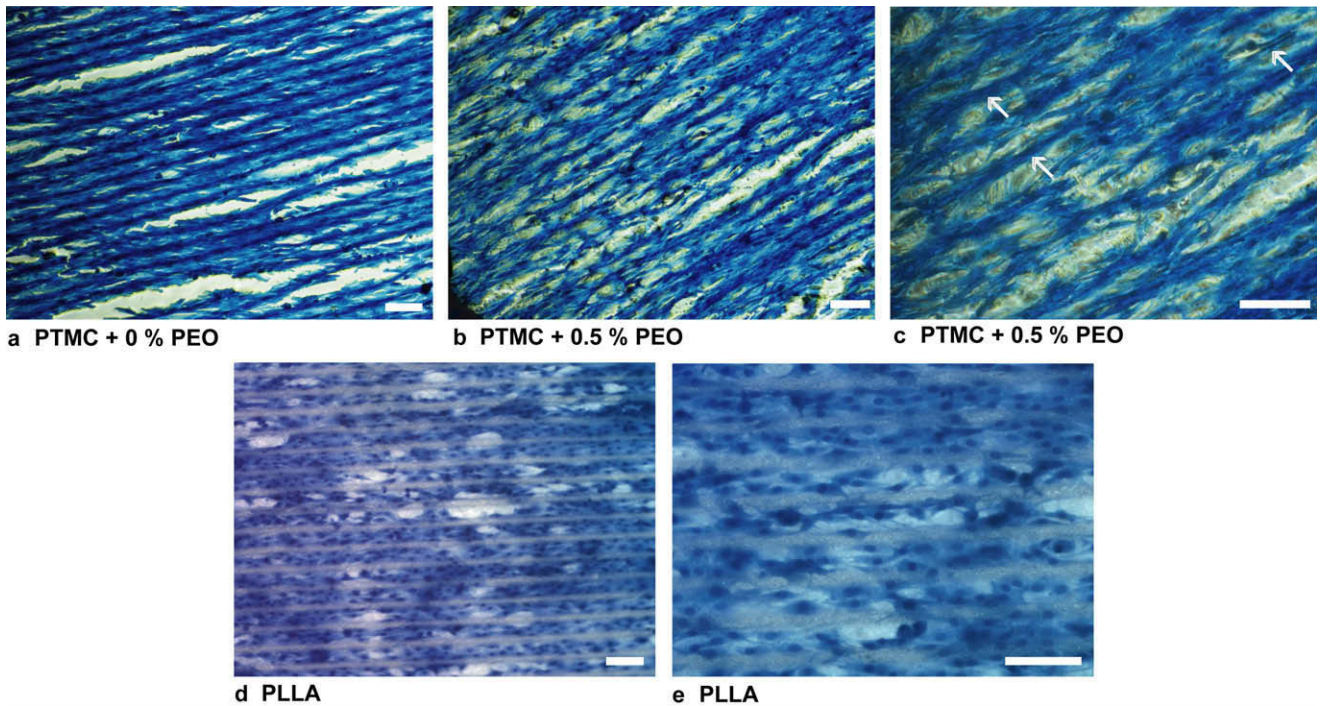


Fig. 6. Light microscopy images of C2C12 cells aligning on PTMC sheets (a–c) and PLLA sheets (d and e) with 25 μm channels. PTMC sheets were cast from (a) 0 wt.% PEO, magnification × 10, (b) 0.5 wt.% PEO solutions, magnification × 10; (c) close-up of image (b) (magnification × 20). All sheets were γ-irradiated. As reference porous PLLA sheets also with 25 μm channels are presented: (d) magnification × 10 and (e) close-up of image (d), magnification × 20. Seeding density of 15,000 cells cm<sup>-2</sup>, 4 days of culturing, bars represent 100 μm, arrows indicate specific cell morphology on PTMC sheets.

### 3.6. Cell proliferation

First, the influence of various parameters of the PTMC sheet fabrication process on the proliferation of C2C12 cells was studied; a DNA assay was performed on cells cultured on different sheets. Porous sheets prepared with 0.5 and 1 wt.% PEO, both non-patterned and micro-patterned, featuring 25  $\mu\text{m}$  wide channels were studied. Additionally,  $\gamma$ -irradiated sheets were included in this study, including non-porous PTMC sheets without PEO, to determine the effect of porosity under unchanged fabrication conditions.

Fig. 7 presents the DNA concentrations on day 4 for the standard (Fig. 7a) and irradiated sheets (Fig. 7b) with respect to the corresponding values for TCPS. The results for the standard sheets indicated a decrease in cell proliferation with increasing PEO content in the polymer solution. Both patterned as well as non-patterned sheets cast from the 1 wt.% PEO showed a significant decrease in cell prolifer-

ation compared with TCPS, as did the patterned sheets from the 0.5 wt.% PEO solution. For the  $\gamma$ -irradiated sheets, with low porosity, only the patterned sheets cast from the 1 wt.% PEO solution showed a significant decrease compared with TCPS. All other sheets exhibited similar DNA concentrations (Fig. 7b). Comparison of the standard with the non-irradiated sheets indicated a significant decrease only for the patterned sheets cast from the 1 wt.% PEO solution.

Combined, the results suggest that the high porosity of the standard sheets seems to affect cell proliferation, whereas neither the residual PEO in the sheets nor irradiation seemed to have any effect.

To study the effect of porosity in these PTMC sheets in more detail, cell attachment and proliferation (by trypan blue exclusion and count) up to 8 days was determined for sheets prepared with 0.75 wt.% versus 0 wt.% PEO using, besides TCPS, dense and porous PLLA sheets as ref-

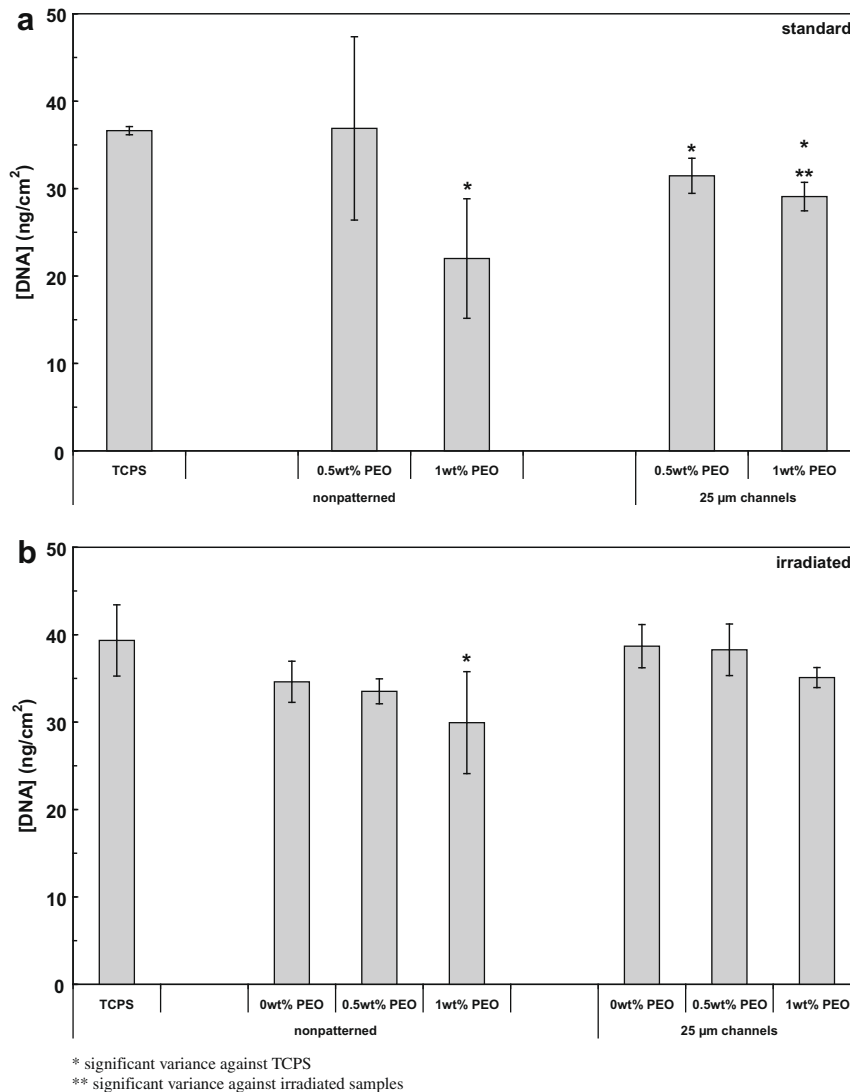


Fig. 7. DNA assay for dense (0 wt.% PEO) and porous (0.5 and 1 wt.% PEO) PTMC sheets with and without pattern for both (a) standard sheets used shortly after casting, washing and drying and (b) sheets that were subsequently  $\gamma$ -irradiated. Seeding density was 15,000 cells  $\text{cm}^{-2}$  and culture for 4 days. Significance was calculated by a two-tailed *t*-test with  $P < 0.05$ . Error bars indicate standard deviation.

erence materials. Fig. 8a shows that cell attachment to both dense and porous PTMC sheets was comparable with the TCPS and PLLA controls; over 85–95% of the total number of seeded cells were attached within 4 h after seeding. Fig. 8b indicates no significant variation in cell proliferation on PTMC and PLLA sheets compared with TCPS on day 4, but on day 8 proliferation seemed decreased on the porous PTMC sheets when compared with both the TCPS control and the porous PLLA. This observation is in line with the suggested decrease in proliferation on the 1 wt.% PEO sheets on day 4 as presented in Fig. 7a. All other sheets were comparable on day 8. When the percentage of dead cells was analyzed it appeared that the number of dead cells was comparable for all sheets; between 2% and 5% on day 4 and 3–7% on day 8.

These results suggest that neither the type of scaffold material nor the processing conditions but rather another

variable caused the decrease in cell proliferation. The first hypothesis, as also suggested by the cell morphology presented in Fig. 6, could be that the cells exit from the cell cycle and start differentiating into the myogenic lineage. Another explanation could be the influence of porosity and/or surface pores, as suggested by the DNA assay data. Perhaps the cells migrate within the scaffold's large surface pores when reaching higher confluency levels, i.e. for longer culture times. During trypsinization these cells may be entrapped within the scaffold, resulting in lower cell numbers available for counting. In addition, cells which grew into the inner pores might experience decreased levels of nutrients, leading to reduced proliferation rates, when the cells on the surface formed a monolayer.

To test the first hypothesis of differentiation into the myogenic lineage, expression of two markers upregulated during myogenic differentiation was analyzed. Early and

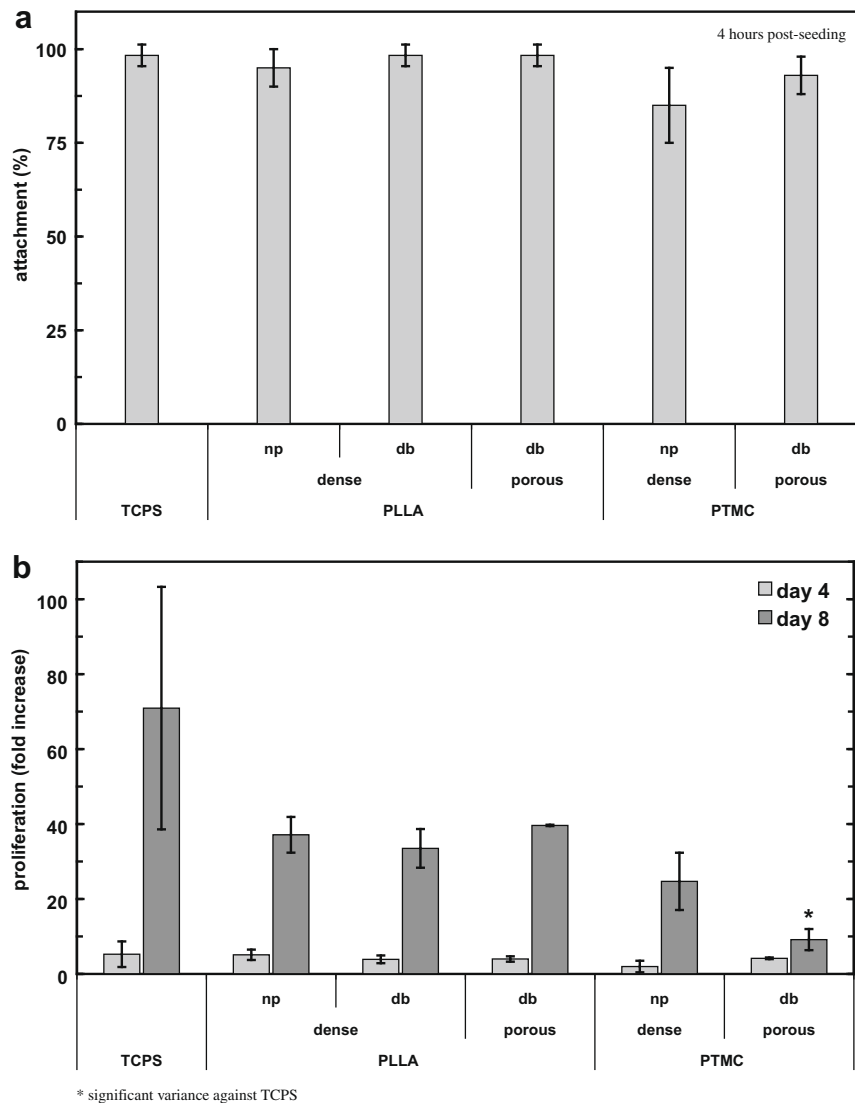


Fig. 8. C2C12 cell behavior with respect to PTMC and PLLA sheets, including TCPS as reference. (a) Attachment 4 h after initial seeding; (b) cell proliferation on days 4 and 8 by trypan blue exclusion. For the porous PTMC sheets a 0.75 wt.% PEO solution was used. np, non-patterned; db, double brick pattern. Seeding density was 15,000 cells cm<sup>-2</sup>. Significance was calculated by a two-tailed *t*-test with *P* < 0.05. Error bars indicate standard deviation.

late myogenesis markers, myoD and myogenin, respectively, were measured on days 4 and 8 for both dense and porous PTMC, with PLLA sheets and TCPS again being used as references. To test the second hypothesis of cell entrapment within the pores the scaffolds were fixed and stained with methylene blue after trypsinization to visualize entrapped cells. Due to the porosity of the scaffolds, and the observed high flux through the porous scaffolds, we assumed that the fixative and staining would easily diffuse through the inner pores of the scaffold and, therefore, stain any remaining cells.

### 3.6.1. Gene expression for myogenic differentiation

Fig. 9 presents the fold induction of myoD and myogenin (myoG) on the various scaffold sheets versus the TCPS control. On day 4 the non-patterned PTMC sheets, both porous and dense, and the patterned dense sheets showed down-regulated expression of myoD (0.3–0.4-fold induction) and myoG (0.1–0.2-fold induction), as do the PLLA non-patterned dense sheets for myoG (0.3-fold induction). The other sheets did not show significant up- or down-regulation on day 4. In general, both myogenesis markers were expressed to a higher extent on day 8 compared with day 4, however, on day 8 the values for the scaffold sheets are more similar to TCPS. On day 8 only the dense non-patterned PTMC sheets still showed significant down-regulation of myoG expression (0.7-fold induction). On the other hand, both the porous and dense micro-patterned PLLA sheets showed an increase in myoD expression (3.1–3.4-fold induction) and the porous sheets also for myoG (2.2-fold induction) compared with TCPS.

From this data it is clear that the apparent decrease in proliferation rate of the cells on the porous PTMC sheets is not due to the activation of the myogenesis pathway. When comparing the porous PTMC sheets with the corre-

sponding dense sheets, significant increased myoD and myoG expression was observed for the patterned sheets on day 4 and non-patterned sheets on day 8. However, all PTMC sheets except for the porous patterned ones inhibited myoD and myoG expression on day 4 compared with TCPS, implying delayed myogenic differentiation. On day 8 these sheets showed similar gene expression levels to the TCPS control except for the dense non-patterned sheets, which still had reduced levels of myoG expression. This phenomenon might suggest that the PTMC material suppresses myogenic differentiation, especially when considering the porous and dense patterned PLLA sheets on day 8, when myoD expression was significantly up-regulated, as was myoG expression for the porous patterned PLLA sheets, suggesting that the double brick pattern applied might activate myogenic differentiation. Although when the patterned sheets were compared with the corresponding non-patterned sheets, only the dense PLLA sheets on day 4 yielded a significant increase in gene expression. The counter-effects of the micro-patterning and porosity might have reversed the inhibitory effect of PTMC on gene expression on the porous patterned PTMC sheets on day 4, leveling the myoD and myoG expression, causing only these porous patterned sheets of all the PTMC sheets to express similar myoD and myoG levels compared with TCPS on day 4. However, this effect is not seen for all patterned and/or porous PTMC sheets and, therefore, more detailed gene expression analysis is necessary to draw any firm conclusions on the exact effect of PTMC, porosity and the double brick pattern on stimulating or suppressing the myogenic pathway in C2C12 cells.

### 3.6.2. Cell entrapment

Fig. 10 presents light microscopy images of a dense non-patterned sheet after 8 days (Fig. 10d) and non-patterned

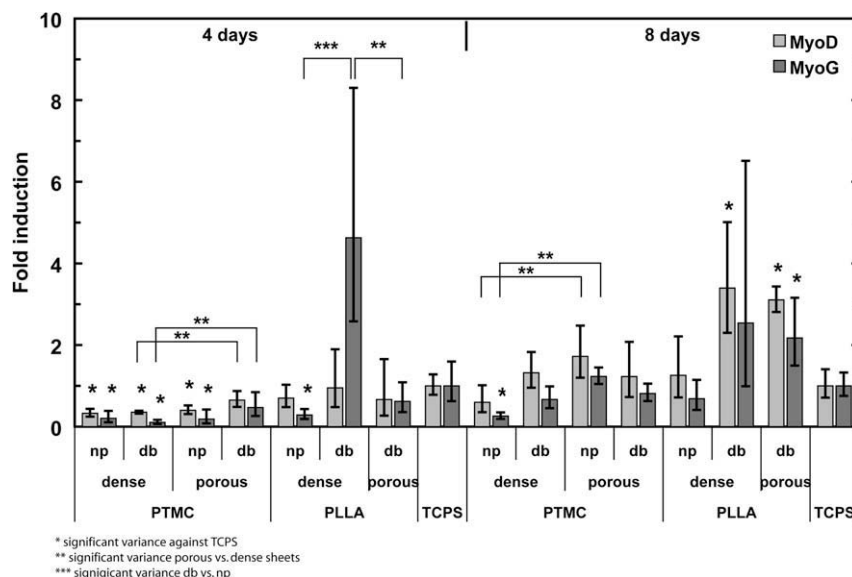


Fig. 9. Quantitative RT-PCR data on myogenesis for the early and late marker myoD and myoG. Fold induction of gene expression with respect to the TCPS control, normalized against GAPDH, as determined by the  $2^{-\Delta\Delta C_T}$  method. np, non-patterned; db, double brick pattern. Seeding density was 15,000 cells  $\text{cm}^{-2}$ . Significance was calculated by a two-tailed *t*-test with  $P < 0.05$ . Error bars indicate standard deviation.

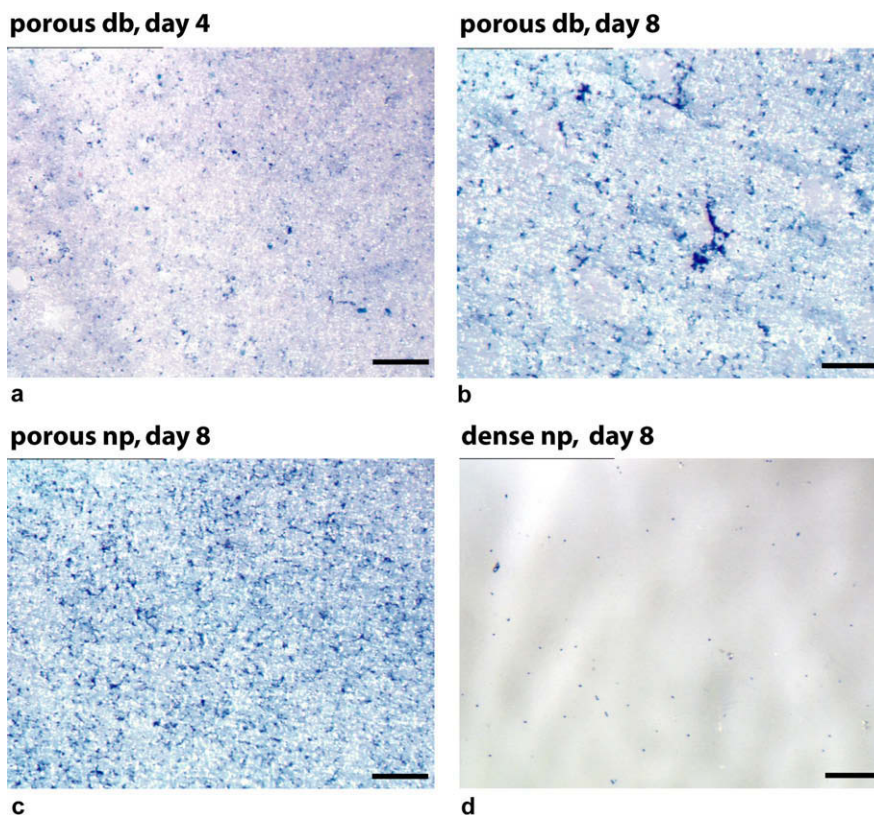


Fig. 10. Light microscope images of PTMC sheets after trypsinization, fixation and staining to visualize remaining cells: (a and b) porous sheet incorporating the double brick pattern on days (a) 4 and (b) 8; (c and d) non-patterned (c) porous and (d) dense sheets on day 8. Magnification  $\times 5$ , the bar represents 200  $\mu\text{m}$ .

and patterned porous sheets after 4 and 8 days (Fig. 10a–c) after trypsinization. A clear contrast between the dense and porous sheets can be observed; cells remain within the porous PTMC sheets whereas no cells remain on the dense sheets after trypsinization, a phenomenon which is more pronounced on day 8 than on day 4. Whether these remaining cells can completely make up for the variation between the dense non-patterned sheet and the porous patterned sheet cannot be concluded from these images. There might be an additional effect of the pores present in the surface reducing the surface area to which the cells can attach, affecting cell growth when cell number rises. Or creep of the PTMC at the surface might affect cell growth, although no drastic morphological changes were observed for sheets incubated in medium for a period similar to the culture period (Fig. 5a). Additionally, no increase in dead cells was seen with the trypan blue exclusion assay, as discussed previously.

#### 4. Conclusions

Porous micro-patterned sheets of flexible and amorphous PTMC were prepared using PS $\mu\text{M}$ . An important finding of this work is the role of PEO as an additive in the pore formation process. PEO seems to induce a highly interconnected porous morphology into otherwise dense sheets by changing the thermodynamic conditions during

the phase separation process. As a result, the PTMC sheets obtained revealed high glucose diffusivity.

Due to the low Young's modulus of PTMC the sheets shrink significantly during fabrication and the pore morphology changes with time under culture conditions. Perhaps co-polymers of PTMC with PLA, which combine the flexibility and good degradation properties of PTMC with the improved mechanical properties of PLA, may be used in future studies to avoid shrinkage of the sheets. Despite their rather low Young's modulus the patterned PTMC sheets were well replicated.

The exact effect of PTMC, porosity and micro-patterning on the activation of myogenic differentiation in C2C12 cells is not completely clear, although there are indications that PTMC might suppress differentiation at first and porosity and micro-patterning might facilitate myogenesis.

The cells attach, align and proliferate well on the surface of PTMC sheets with relatively small pores. Cells partially migrate into the inner pores of PTMC scaffolds with relatively large pores.

#### Acknowledgments

The authors would like to thank Dr J. de Boer and Prof. Dr C.A. van Blitterswijk (Department of Tissue Regeneration, University of Twente, The Netherlands) for facilitating

the cell culture experiments. This project was financially supported by the Spearhead program “Advanced Polymeric Microstructures for Tissue Engineering” of the University of Twente (Institute for Biomedical Technology).

## References

- [1] Murugan R, Ramakrishna S. Design strategies of tissue engineering scaffolds with controlled fiber orientation. *Tissue Eng* 2007;13(8):1845–66.
- [2] Ma PX. Scaffolds for tissue fabrication. *Mater Today* 2004;7(5):30–40.
- [3] Gunatillake PA, Adhikari R. Biodegradable synthetic polymers for tissue engineering. *Eur Cells Mater* 2003;5:1–16.
- [4] Agrawal CM, Ray RB. Biodegradable polymeric scaffolds for musculoskeletal tissue engineering. *J Biomed Mater Res* 2001;55(2):141–50.
- [5] Zhang Z, Kuijter R, Bulstra SK, Grijpma DW, Feijen J. The *in vivo* and *in vitro* degradation behavior of poly(trimethylene carbonate). *Biomaterials* 2006;27(9):1741–8.
- [6] Zhu KJ, Hendren RW, Jensen K, Pitt CG. Synthesis, properties, and biodegradation of poly(1,3-trimethylene carbonate). *Macromolecules* 1991;24(8):1736–40.
- [7] Pêgo AP, Grijpma DW, Feijen J. Enhanced mechanical properties of 1,3-trimethylene carbonate polymers and networks. *Polymer* 2003;44(21):6495–504.
- [8] Edlund U, Albertsson AC. Degradable polymer microspheres for controlled drug delivery. *Degradable aliphatic polyesters*. Berlin: Springer Verlag; 2001.
- [9] Engelberg I, Kohn J. Physico-mechanical properties of degradable polymers used in medical applications: a comparative study. *Biomaterials* 1991;12(3):292–304.
- [10] Jia Y, Shen X, Gu X, Dong J, Mu C, Zhang Y. Synthesis and characterization of tercopolymers derived from  $\epsilon$ -caprolactone, trimethylene carbonate, and lactide. *Polym Adv Technol* 2008;19(2):159–66.
- [11] Zhang Z, Grijpma DW, Feijen J. Triblock copolymers based on 1,3-trimethylene carbonate and lactide as biodegradable thermoplastic elastomers. *Macromol Chem Phys* 2004;205(7):867–75.
- [12] Chapanian R, Tse MY, Pang SC, Amsden BG. The role of oxidation and enzymatic hydrolysis on the *in vivo* degradation of trimethylene carbonate based photocrosslinkable elastomers. *Biomaterials* 2009;30(3):295–306.
- [13] Qin Y, Yuan M, Li L, Guo S, Yuan M, Li W, et al. Use of polylactic acid/polytrimethylene carbonate blends membrane to prevent post-operative adhesions. *J Biomed Mater Res Part B-Appl Biomater* 2006;79B(2):312–9.
- [14] Yang S, Leong K-F, Du Z, Chua C-K. The design of scaffolds for use in tissue engineering. Part I. Traditional factors. *Tissue Eng* 2001;7(6):679–89.
- [15] Lim JY, Donahue HJ. Cell sensing and response to micro- and nanostructured surfaces produced by chemical and topographic patterning. *Tissue Eng* 2007;13(8):1879–91.
- [16] Khademhosseini A, Langer R, Borenstein J, Vacanti JP. Tissue engineering special feature: microscale technologies for tissue engineering and biology. *PNAS* February 21, 2006;103(8):2480–7.
- [17] Papenburg BJ, Vogelaar L, Bolhuis-Versteeg LAM, Lammertink RGH, Stamatiadis D, Wessling M. One-step fabrication of porous micropatterned scaffolds to control cell behavior. *Biomaterials* 2007;28(11):1998–2009.
- [18] Vogelaar L, Barsema JN, Rijn CJMv, Nijdam W, Wessling M. Phase separation micromolding – PS $\mu$ M. *Adv Mater* 2003;15(16):1385–9.
- [19] Livak KJ, Schmittgen TD. Analysis of relative gene expression data using real-time quantitative PCR and the 2- $^{-\Delta\Delta CT}$  method. *Methods* 2001;25(4):402–8.
- [20] Pego AP, Poot AA, Grijpma DW, Feijen J. Copolymers of trimethylene carbonate and epsilon-caprolactone for porous nerve guides: synthesis and properties. *J Biomater Sci-Polym Ed* 2001;12(1):35–53.
- [21] Wienk IM, Boom RM, Beerlage MAM, Bulte AMW, Smolders CA, Strathmann H. Recent advances in the formation of phase inversion membranes made from amorphous or semi-crystalline polymers. *J Membrane Sci* 1996;113(2):361–71.
- [22] Saltzman WM. *Tissue engineering: principles for the design of replacement organs and tissues*. 1st ed. Oxford: Oxford University Press; 2004.
- [23] Tannu NS, Rao VK, Chaudhary RM, Giorgianni F, Saeed AE, Gao Y, et al. Comparative proteomes of the proliferating C2C12 myoblasts and fully differentiated myotubes reveal the complexity of the skeletal muscle differentiation program. *Mol Cell Proteom*, 2004;3(11):1065–82.
- [24] Grossi A, Yadav K, Lawson MA. Mechanical stimulation increases proliferation, differentiation and protein expression in culture: stimulation effects are substrate dependent. *J Biomech* 2007;40(15):3354–62.
- [25] Lan MA, Gersbach CA, Michael KE, Keselowsky BG, García AJ. Myoblast proliferation and differentiation on fibronectin-coated self assembled monolayers presenting different surface chemistries. *Biomaterials* 2005;26(22):4523–31.
- [26] Boonthekul T, Hill EE, Kong HJ, Mooney DJ. Regulating myoblast phenotype through controlled gel stiffness and degradation. *Tissue Eng* 2007;13(7):1431–42.
- [27] Yoshida N, Yoshida S, Koishi K, Masuda K, Nabeshima Y. Cell heterogeneity upon myogenic differentiation: down-regulation of MyoD and Myf-5 generates “reserve cells”. *J Cell Sci*, 1998;111(6):769–79.